



**HAL**  
open science

## Preparation of miniaturized hydrophilic affinity monoliths: Towards a reduction of non-specific interactions and an increased target protein density

Julie GIL, Isabelle Krimm, Vincent Dugas, Claire Demesmay

### ► To cite this version:

Julie GIL, Isabelle Krimm, Vincent Dugas, Claire Demesmay. Preparation of miniaturized hydrophilic affinity monoliths: Towards a reduction of non-specific interactions and an increased target protein density. *Journal of Chromatography A*, 2023, 1687, pp.463670. 10.1016/j.chroma.2022.463670 . hal-03888930

**HAL Id: hal-03888930**

**<https://hal.science/hal-03888930>**

Submitted on 7 Dec 2022

**HAL** is a multi-disciplinary open access archive for the deposit and dissemination of scientific research documents, whether they are published or not. The documents may come from teaching and research institutions in France or abroad, or from public or private research centers.

L'archive ouverte pluridisciplinaire **HAL**, est destinée au dépôt et à la diffusion de documents scientifiques de niveau recherche, publiés ou non, émanant des établissements d'enseignement et de recherche français ou étrangers, des laboratoires publics ou privés.

1 Preparation of miniaturized hydrophilic affinity monoliths: towards a  
2 reduction of non-specific interactions and an increased target protein  
3 density

4  
5 Julie GIL<sup>1</sup>, Isabelle Krimm<sup>2</sup>, Vincent Dugas<sup>1</sup>, Claire Demesmay<sup>1</sup>

6  
7  
8 *1 – Université de Lyon, CNRS, Université Claude Bernard Lyon 1, Institut des Sciences Analytiques, UMR 5280, 5*  
9 *rue de la Doua, F-69100 VILLEURBANNE, France*

10 *2 – Université de Lyon, Université Claude Bernard Lyon 1, INSERM 1052, CNRS 5286, Centre Léon Bérard, Centre*  
11 *de recherche en cancérologie de Lyon, Small Molecules for Biological Targets Team, Lyon, 69373, France*

12

13

14

15

16

17

18 Keywords

19 Frontal affinity chromatography, hydrophilic organic monolith, non-specific interactions, fragment  
20 screening

21

22

## 23 Abstract

24 In affinity chromatography, non-specific interactions between the ligands and the affinity column may  
25 affect the results, leading to misinterpretations during the investigation of protein-ligand interactions  
26 (detection of false positives in ligand screening, lack of specificity in purification). Such non-specific  
27 interactions may arise both from the underlying support or from the target protein itself. If the second  
28 ones are protein-dependent (and cannot be studied in a general framework), the first ones occur in  
29 the same way regardless of the immobilized target. We propose a methodology to identify the origin  
30 of such non-specific interactions with the underlying material of the affinity column. This methodology  
31 relies on the systematic investigation of the retention behavior of a set of 41 low-molecular weight  
32 compounds covering a wide chemical space (net charge, log D, functionality). We first demonstrate  
33 that the main source of non-specific interactions on the most commonly used GMA-co-EDMA monolith  
34 comes from hydrophobic effects. To reduce such non-specific interactions, we developed a new  
35 hydrophilic glycidyl methacrylate-based monolith by replacing the EDMA crosslinker by the more  
36 hydrophilic N-N' Methylenebisacrylamide (MBA). Optimization of the synthesis parameters (monomer  
37 content, initiation type, temperature) has focused on the reduction of non-specific interaction with  
38 the monolithic support while maximizing the amount of protein that can be grafted onto the monolith  
39 at the issue of its synthesis. The retention data of the 41 test solutes on the new poly(GMA-co-MBA)  
40 monolith shows a drastic reduction of non-specific interactions except for cationic compounds. The  
41 particular behavior of cationic compounds is due to their electrostatic interactions with carboxylic  
42 groups resulting from the partial acidic hydrolysis of amide groups of MBA during the epoxide ring  
43 opening step. So, the ring opening step in acidic media was replaced by a hot water treatment to avoid  
44 side reaction on MBA. The new monolith poly(GMA-co-MBA) not only has improved hydrophilic  
45 surface properties but also a higher protein density ( $16 \pm 0.8 \text{ pmol cm}^{-1}$  instead of  $8 \pm 0.3 \text{ pmol cm}^{-1}$ ).  
46 To highlight the benefits of this new hydrophilic monolith for affinity chromatographic studies, frontal  
47 affinity chromatography experiments were conducted on these monoliths grafted with con A.

48

## 49 1- Introduction

50 Affinity monolith chromatography (AMC) is a type of liquid chromatography that uses monolithic  
51 supports functionalized with biological targets such as proteins, receptors, antibodies or enzymes [1–  
52 3]. AMC is a powerful method for clean-up and preconcentration purposes in sample treatment [4,5],  
53 chiral separation [6] and ligand or fragment screening in Drug discovery [7,8]. Applications also include  
54 the study of biological interactions to get information on the stoichiometry, thermodynamics and  
55 kinetics of the interaction between the immobilized biological target and ligands in solution.

56 Miniaturized affinity monolith chromatography  $\mu$ AMC, with columns in the few tens  $\mu$ m range covers  
57 all the application fields of AMC with the tremendous advantage of reducing the quantity of biological  
58 material to be immobilized.

59 Several reasons have driven the development of miniaturized affinity chromatography with monolithic  
60 supports. First, these supports are synthesized *in-situ* as continuous bed supports avoiding the  
61 cumbersome filling of columns with particles. Their external porosity can be tuned to increase their  
62 permeability and decrease back pressures thus allowing higher flow rates (useful for increasing the  
63 throughput in screening campaigns, for decreasing the percolation time in purification or clean up  
64 applications). Whatever the application field, the underlying monolithic material supporting the  
65 biomolecules must satisfy two main criteria: the quantity of protein per unit volume must be as high  
66 as possible and its intrinsic capacity to limit non-specific interactions. The quest for a stealthy  
67 underlying support in affinity chromatography is a complex and difficult task [9,10].

68 Organic monoliths are usually preferred to their silica counterparts for their easier preparation  
69 (thermally or photochemically initiated polymerization). Moreover the great diversity of  
70 commercially available monomers allows tuning their surface properties and adjusting available  
71 functional moieties for their subsequent grafting with a biological target [11]. They also usually offer a  
72 satisfactory mechanical resistance and a tunable permeability allowing their *in-line* coupling with  
73 another separation dimension (liquid chromatography or capillary electrophoresis) [12–14]. A great  
74 diversity of organic monoliths has been synthesized. Among those, GMA-co-EDMA monoliths have  
75 found applications in many areas (for the preparation of IMERS dedicated to *on-line* solid-supported  
76 enzymatic digestion, immunoaffinity preconcentration, separation...)[12,15–17]. Moreover, their  
77 synthesis is well-documented, they present a satisfactory chemical and thermal stability, and their  
78 surface epoxy groups open multiple grafting-ways to prepare a wide range of stationary phases, from  
79 ion-exchange to affinity columns through biomolecules immobilization (*e.g.*, aptamers and proteins).

80 Despite their frequent use, there is very little information on the non-specific interactions generated  
81 by these GMA-co-EDMA monolithic based stationary phases. During a previous ligand/protein  
82 interaction study by AMC [7], we have noticed that non-specific interactions can be non negligible  
83 when these GMA-co-EDMA monoliths are used as underlying material for affinity columns. Indeed,  
84 GMA-co-EDMA monoliths are used in experimental conditions close to physiological conditions (purely  
85 aqueous medium at pH 7.4, with high salt concentration) favoring secondary interactions by  
86 hydrophobic effect. We have shown that such non-specific interactions occur regardless of the mode  
87 of grafting but are of less importance after grafting according to the Schiff base method *i.e.*, when  
88 residual reduced aldehyde groups remain at the monolith surface instead of epoxy ones even after

89 end-capping. The existence of such interactions can lead to (i) a lack of specificity/recovery if they are  
90 used for purification/preconcentration, (ii) a lack of recovery of the products resulting from the  
91 enzymatic digestion (for IMERS), (iii) the detection of false positives in the case of ligand screening and  
92 to (iv) a misestimation of thermodynamics parameters such as affinity constant determination.  
93 Because non-specific interactions are a concern in bioaffinity chromatography, their characterization  
94 seems a prerequisite to any stationary phase optimization. To our knowledge, sources of non-specific  
95 interactions with the underlying support on affinity monoliths have not been thoroughly investigated.  
96 For instance, no dedicated method was developed and accepted to characterize the level and origin of  
97 non-specific interactions of small molecules on monolithic phases used as chromatographic underlying  
98 support for affinity columns.

99 Our study stems on improving the conditions for detecting low affinities in affinity chromatography by  
100 reducing unwanted interactions with the chromatographic support. In a preliminary investigative  
101 study, we report a methodology aiming at characterizing non-specific interactions due to the- GMA-  
102 co-EDMA underlying material widely used for the preparation of affinity columns. To achieve this task,  
103 we selected a set of 41 molecules from a library of fragment-like molecules covering the whole range  
104 of physico-chemical properties in terms of net charge, logD, H-bond donor and acceptor. The physical-  
105 chemical properties and chemical structures of the set of fragments are detailed in Table S1. Based on  
106 the outcomes of the preliminary study (non-specific interactions mainly due to hydrophobic effects),  
107 we propose the synthesis of a new glycidyl based monolith, by using MBA crosslinker (instead of EDMA)  
108 to increase the hydrophilicity of the resulting monolith. Both the grafting capacity and the surface  
109 properties regarding the non-specific interactions of the newly prepared monolith are optimized and  
110 characterized. Non-specific interactions are characterized using the developed methodology based on  
111 the library of small chemical compounds. The grafting capacity is evaluated by determining the amount  
112 of biological active sites present at the monolith surface after the grafting of a biological target onto  
113 the monolith (amount of sites able to bind a ligand of known activity). Streptavidin is used as model  
114 target protein and HABA as a test ligand. Finally, to evaluate the improvement of the new monolith in  
115 affinity chromatography, low affinity ligands are used on a Concanavalin A grafted monolith. These  
116 experiments highlight the benefits associated with reduced non-specific interactions and an increased  
117 target protein density. All these experiments are carried out by frontal affinity experiments (with a  
118 dedicated in-house developed instrumentation [18]) as described in the Material and Methods  
119 Section.

120

121

122 2- Material and methods

123 2.1- Reagents and Buffers.

124 Streptavidin (from *Streptomyces avidinii*, affinity purified,  $\geq 13$  U  $\text{mg}^{-1}$  of protein), Concanavalin A (Con  
125 A) from *Canavalia ensiformis*, (3-methacryloxypropyl)-trimethoxysilane ( $\gamma$ -MAPS), ethylene  
126 dimethacrylate (EDMA), glycidyl methacrylate (GMA), acrylamide, N,N'-Methylenebis(acrylamide)  
127 (MBA), Acrylamide (AA), 1-propanol, 1,4-butanediol, dimethyl sulfoxide (DMSO), sodium periodate,  
128 lithium hydroxide, dipotassium hydrogen phosphate ( $\text{K}_2\text{HPO}_4$ ), o-phosphoric acid, sulfuric acid, sodium  
129 cyanoborohydride, triethylamine (TEA), azobis(isobutyronitrile) (AIBN), 4'-Hydroxyazobenzene-2-  
130 carboxylic acid (HABA), p-nitrophenyl- $\alpha$ -D-mannopyranoside ( $\alpha$ PNM), p-nitrophenyl- $\alpha$ -D-  
131 glucopyranoside ( $\alpha$ PNG) and p-nitrophenyl- $\alpha$ -D-galactopyranoside ( $\alpha$ PNGal) and ligands (Table S1)  
132 were purchased from Sigma-Aldrich (L'Isle d'Abeau Chesne, France). All aqueous solutions were  
133 prepared using  $>18$  M $\Omega$  deionized water. Phosphate buffer was prepared by dissolving 1.17 g of  $\text{K}_2\text{HPO}_4$   
134 in 100 mL of ultrapure water and the pH was adjusted to 7.4 with phosphoric acid.

135 2.2- Monolithic capillary column synthesis

136 Fused-silica capillaries with UV transparent coating (TSH, 75- $\mu\text{m}$  i. d.) or polyimide coating (TSP, 75- $\mu\text{m}$   
137 i.d.) were purchased from Polymicro Technologies (Molex). In all cases, capillaries were pre-treated by  
138 flushing capillaries with a 5% (v/v) solution of  $\gamma$ -MAPS in methanol/water (95/5, v/v) with 2.5% TEA for  
139 1 h at 7 bar. Next, they were rinsed with methanol for 15 min at 7 bar and dried at room temperature  
140 under nitrogen stream.

141 2.2.1 GMA-co-EDMA Monolith synthesis:

142 Poly(GMA-co-EDMA) monoliths were synthesized as described in a previous work [7]. The  
143 polymerization mixture was prepared by mixing 0.9 mL GMA, 0.3 mL EDMA, 1.05 mL 1-propanol, 0.6  
144 mL 1,4-butanediol, 0.15 mL ultra-pure water and 12 mg of AIBN initiator. The pre-treated capillary (TSH  
145 Capillary) was then filled with the polymerization mixture under 1 bar  $\text{N}_2$  pressure. The  
146 photopolymerization reaction was performed in a Bio-link UV cross-linker (VWR International, France)  
147 under 365 nm UV light for a total energy of 6  $\text{J cm}^{-2}$ . To localize the monolith inside the silica capillary,  
148 a PEEK tubing (380  $\mu\text{m}$  i. d.) was used as a mask to cover non-irradiated areas. After polymerization,  
149 the capillary was rinsed with methanol for 1 h.

150 2.2.2 GMA-co-MBA monolith synthesis

151 Poly(GMA-co-MBA) monoliths were prepared as follows, adapting protocols from [19]. First, a mixture  
152 of solvents was prepared by mixing 3330 mg of DMSO, 1480 mg of 1,4-butanediol and 1850 mg of

153 dodecanol. Then, 320 mg of MBA were added and sonicated 1 h at room temperature. After the  
154 dissolution of MBA, 480 mg of GMA were added and sonicated 1 h at room temperature. 8 mg of AIBN  
155 were added and the final mixture was sonicated 15 min at room temperature. The pre-treated capillary  
156 (TSP Capillary) was then filled with the polymerization mixture under 1 bar N<sub>2</sub> pressure and the ends  
157 of the capillary sealed. The polymerization reaction was performed in water bath at 57°C for 18 hours.  
158 After polymerization monoliths were rinsed with methanol for 1 h.

### 159 2.3 Protein (streptavidin) immobilization

160 Streptavidin was grafted using the Schiff base method as previously described [7]. First, the epoxy  
161 groups of the GMA-co-EDMA monoliths were hydrolyzed into diols flowing 1 M sulfuric acid for 2 h at  
162 7 bar. After water rinsing, the diol-monolith was oxidized to aldehyde using a 0.12 M NaIO<sub>4</sub> solution at  
163 pH 5.5. Then, a 1 mg mL<sup>-1</sup> Streptavidin and 4 mg mL<sup>-1</sup> NaBH<sub>3</sub>CN solution in 67 mM phosphate buffer  
164 (pH 6) was percolated through the column for 18 h at 7 bar and room temperature. After  
165 immobilization, the column was flushed with sodium borohydride (2.5 mg mL<sup>-1</sup>, phosphate buffer 67  
166 mM pH 8) (2 h, 7 bar) to reduce residual aldehydes. The Streptavidin columns were then rinsed with  
167 phosphate buffer and stored at 4 °C.

### 168 2.4 Nano-FAC experiments

169 Nano-FAC Setup. Frontal Weak Affinity Chromatography experiments were carried out with a 7100  
170 capillary electrophoresis Agilent system (Agilent Technologies, Waldbronn, Germany) equipped with  
171 an external nitrogen tank to reach pressures up to 12bar. System control and data acquisition were  
172 carried out using the Chemstation software (Agilent). All experiments were carried out in “short-end”  
173 injection mode, with the inlet of the capillary immersed in the solution to be infused, so that by  
174 applying external pressure at 12bar the liquid is forced to flow inside the capillary column. The  
175 detection was achieved *in-situ* on an empty section of the column, right after the end of the monolith,  
176 thanks to a diode array detector operated in multi-wavelength mode. [18] The revelation window on  
177 the capillary was obtained by burning away the external coating of the capillary. The analyses were all  
178 carried out under controlled room temperature at 25°C.

#### 179 2.4.1 FAC for the evaluation of non-specific interactions

180 Non-specific interactions were evaluated by infusing compounds individually (100 μM solutions  
181 prepared in phosphate buffer, 67 mM, pH=7,4) on the reduced aldehyde monolithic support until the  
182 breakthrough time was reached. The columns were rinsed for 30 min in-between each infusion. The  
183 breakthrough time is measured for each compound. In the case of non-specific interactions, this  
184 breakthrough time  $t_{\text{breakthrough}}$  is independent of the solute concentration [L] provided this

185 concentration is low enough to work is the linear range of the adsorption isotherm. If no non-specific  
186 interactions take place, the breakthrough time occurs at the dead time (the reduced breakthrough  
187 time is equal to 1). If non-specific interactions occur, the solute is captured by the support until the  
188 equilibrium is reached, and the breakthrough time  $t_{breakthrough}$  is delayed. The higher the non-specific  
189 interactions, the higher the quantity of solute captured and the higher the breakthrough time.

$$190 \quad q_{capt} = (t_{breakthrough} - t_0) * F * [L] = \frac{(t_{breakthrough} - t_0)}{t_0} * V_0 * [L] = k_{ns} * V_0 * [L]$$

191 Where F is the flow rate,  $t_0$  the dead time,  $V_0$  the dead volume of the column and  $k_{ns}$  the retention  
192 factor of the solute due to non-specific interactions.

### 193 2.4.2 Quantification of the number of protein active sites

194 For the determination of the amount of streptavidin active sites available after grafting, HABA ( $K_d =$   
195  $100 \mu\text{M}$ ) was infused as test solute with increasing concentrations (5, 10, 50, 100 and  $200 \mu\text{M}$  solutions  
196 prepared in phosphate buffer, 67 mM,  $\text{pH}=7,4$ ), without any rinsing step in-between the percolation  
197 of different concentrations (staircase experiments). The amount of ligand captured at each step is  
198 determined and the cumulated amount of ligand captured is calculated by summing the captured  
199 quantity at all the steps. The double reciprocal plot showing the amount of ligand captured vs the  
200 ligand concentration allows for the simultaneous determination of both the  $K_d$  value of the  
201 target–ligand interaction and the number of active sites available (Bact) (see S1 for the rationale of the  
202 staircase approach). Rationality of the results was ensured by comparing the obtained  $K_d$  value (range  
203  $90\text{-}120 \mu\text{M}$ ) with literature values ( $100 \mu\text{M}$ ).

204

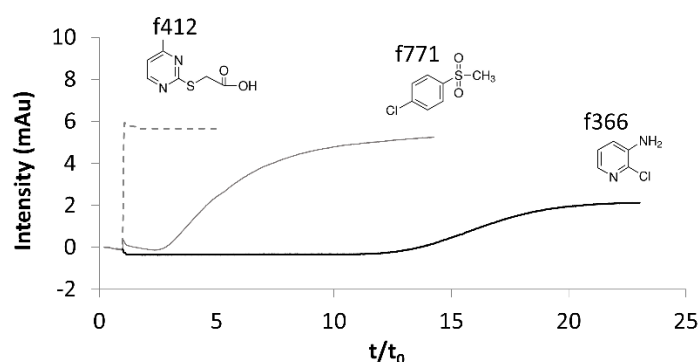
## 205 3- Results and discussion

### 206 3.1 Investigation of non-specific interactions on GMA-co-EDMA monoliths

207 The starting monolith uses glycidyl methacrylate (GMA) as functional monomer and ethylene  
208 dimethacrylate (EDMA) as crosslinker. Preparation of (bio)affinity monoliths requires their subsequent  
209 functionalization with target (bio)molecules such as proteins. The preferred functionalization pathway  
210 implements the hydrolysis of epoxides, followed by the periodate-mediated oxidation of the resulting  
211 diols into aldehyde reactive groups. The protein is then covalently grafted onto the monolith via Schiff  
212 base method. The remaining aldehyde groups after the grafting step are reduced to form alcohol  
213 groups (Figure S2). This biofunctionalization method gives more hydrophilic stationary phases  
214 compared to the one obtained by direct grafting of proteins onto the GMA-based monolith [7]. In  
215 addition, the reaction is faster and results in improved grafting protein densities compared to the

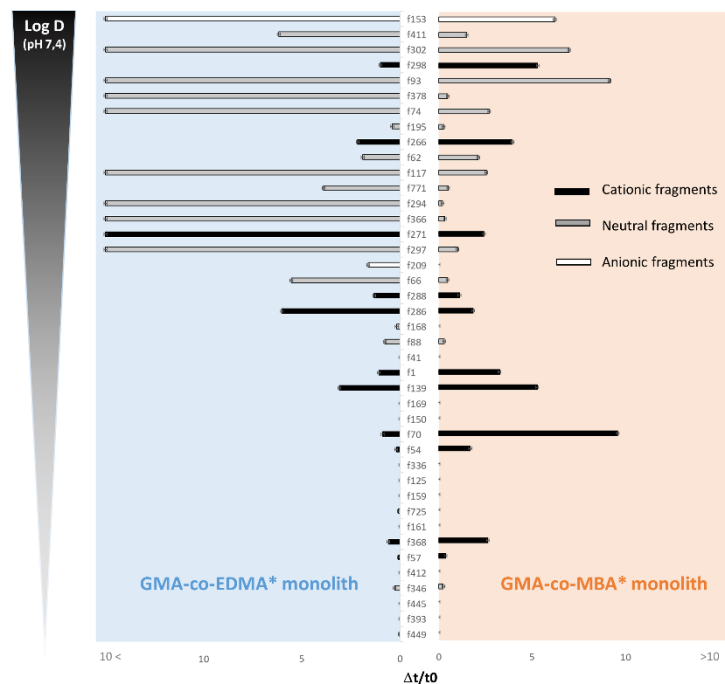


216 epoxy method [20,21]. Using a 75- $\mu\text{m}$  inner diameter capillary, up to  $8 \pm 0.3$  pmol of active streptavidin  
217 binding sites per cm of monolith are reached. The investigation of non-specific interactions on GMA-  
218 co-EDMA based monoliths (interactions with the underlying material and not the whole affinity  
219 column) was carried out on GMA-co-EDMA monoliths subjected to the entire functionalization process  
220 except for the protein grafting step, viz on reduced aldehyde GMA-co-EDMA monoliths. Figure 1  
221 presents the breakthrough curves obtained by nano-FAC experiments for three different molecules of  
222 the library solubilized in a 67 mM phosphate buffer at pH=7,4. For f412, non-specific interactions are  
223 not observed, and the breakthrough time is equal to the dead time ( $k=0$ ). The presence of non-specific  
224 interactions between the ligands and the stationary phase is observed by a shift of the breakthrough  
225 curve from the dead time. The higher the non-specific interactions the higher the breakthrough times  
226 as for f771 (a moderately retained compound,  $k=3.9$ ) and f366 (a highly retained compound  $k=14.7$ )  
227 (Figure 1).



228  
229 Figure 1. Nano-FAC-UV chromatograms of three molecules exhibiting different retention behavior on  
230 the reduced aldehyde GMA-co-EDMA monolith. Ligands were infused in pH 7.4 phosphate buffer  
231 solution at 67 mM and detected at 230, 254 and 280 nm, respectively for f771, f412 and f366.

232  
233 The retention factors (reduced breakthrough times) measured for the 41 molecules are ranked in  
234 ascending order of their logarithm value of the distribution coefficient ( $\log D$ ). All the experiments  
235 were carried out in purely aqueous mobile phase at pH 7.4, i.e., in the experimental conditions  
236 classically used for affinity studies. Results are summarized in Figure 2 (left).



237

238 Figure 2. Bar graphs of the reduced breakthrough times for the 41 molecules on reduced aldehyde  
 239 GMA-co-EDMA\* monolith (left) and reduced aldehyde GMA-co-MBA\* monolith (right).

240

241 The ranking of the fragments according to their  $\log D$  value (at pH 7.4) allows to feature the correlation  
 242 between the retention and the hydrophobic character of test compounds, whatever the net charge of  
 243 the molecules (Figure 2 left). Classification of the ligands according to other molecular or  
 244 physicochemical properties (the whole molecular descriptors used are listed in table S1) did not reveal  
 245 any other correlation. So, despite efforts to limit hydrophobicity of this monolithic stationary phase,  
 246 non-specific interactions seem to be mainly governed by hydrophobic effects. Reducing these  
 247 undesirable interactions involves increasing the hydrophilicity of the monolithic support. Two  
 248 strategies have thus been considered: replacing the EDMA with a more hydrophilic crosslinker (MBA)  
 249 and/or substituting part of the GMA functional monomer with a more hydrophilic monomer such as  
 250 acrylamide [19] at the risk of reducing the amount of active epoxy groups *i.e.* the amount of protein  
 251 that can be immobilized on the monolith.

252

### 253 3.2 Synthesis and characterization of GMA-co-MBA monoliths

254 Synthesis of GMA-co-MBA monoliths was carried out on the basis on the work of Zhu et al [19]. In this  
 255 work, hydrophilic GMA-based monoliths were prepared using N, N' methylenebis(acrylamide) (MBA,  
 256  $\log P$  -1.44) as crosslinker and acrylamide (AA,  $\log P$  -0.77) as co- functional monomer with GMA ( $\log P$

257 1.39). Although monolithic structures were easily obtained in our laboratory using the recipe proposed  
 258 by Zhu [19], the quantity of active proteins measured after grafting (less than 1 pmol cm<sup>-1</sup>) was  
 259 significantly lower than on our GMA-co-EDMA monolith (to 8 ± 0.3 pmol cm<sup>-1</sup>). The optimization of the  
 260 monolith synthesis parameters (e.g., polymerization mixture composition, temperature and  
 261 polymerization time) was undergone to increase the density of active protein that can be grafted on  
 262 the monolithic stationary phase. Assuming the limiting factor is the density of glycidyl reactive groups  
 263 on the monolithic surface, the GMA/AA/MBA monomer ratio was modified, the porogen to monomer  
 264 ratio being kept constant (Table 1). GMA content was increased by decreasing acrylamide and MBA  
 265 content. The optimization criteria of the GMA-co-MBA monolith synthesis was based on the ability to  
 266 still obtain a monolith structure with a satisfactory permeability and on the quantity of active protein  
 267 that could be grafted. Best conditions of the thermally initiated polymerization (18 hours at 57 °C)  
 268 gives rise to a quantity of immobilized active protein of 13 ± 0.8 pmol per cm of monolith. This is a big  
 269 improvement over the initial monolith described by Zhu [19] and the GMA-co-EDMA monolith (8 ± 0.3  
 270 pmol cm<sup>-1</sup>).

271 **Table 1. Comparison of the monomer composition of the GMA-co-MBA polymerization mixture of the initial recipe and**  
 272 **after optimization in this work to increase the active protein density.**

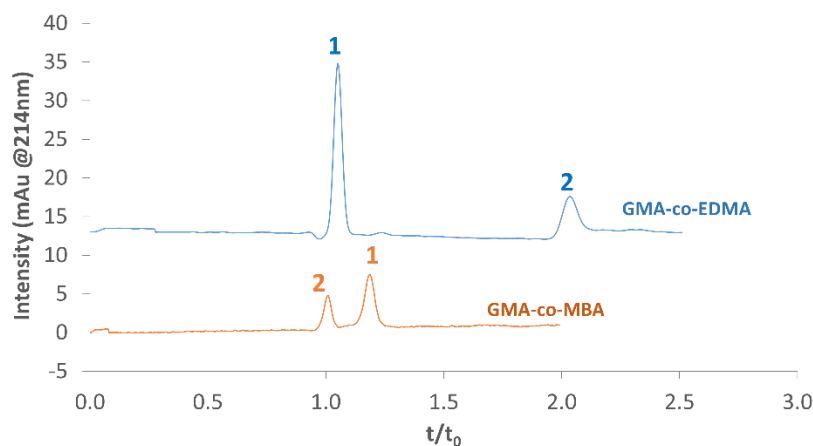
<b>% monomer (w/w)</b>	<b>GMA-co-MBA [19]</b>	<b>GMA-co-MBA This work</b>
GMA	24.8	60
Acrylamide	21.9	0
N,N'-methylenebis(acrylamide)	53.3	40

273

274 Although the protein content is a key parameter, our first goal was to increase the hydrophilicity of  
 275 the monolith. This was evaluated by following the retention behavior of two tests solutes (thiourea a  
 276 polar test solute with a log P value of -1.08 and octylbenzene a highly hydrophobic test solute with a  
 277 log P value of 6.6 in an acetonitrile /water (70:30, v:v) mobile phase. The two chromatograms are  
 278 illustrated Figure 3.

279

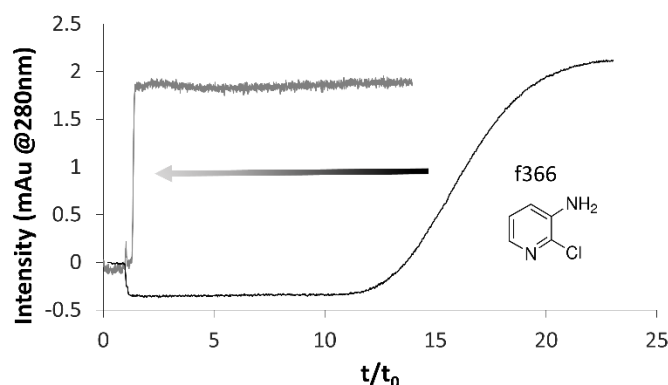
280



281  
 282 Figure 3. Chromatograms of two test solutes on GMA-co-EDMA and GMA-co-MBA monoliths. Solutes :  
 283 Injection of thiourea (1) and octylbenzene (2) in acetonitrile/water (70/30, v :v) mobile phase. UV  
 284 detection at 254 nm. Applied pressure 12 bars.

285  
 286 In these mobile phase conditions (acetonitrile /water, 70:30, v:v), the elution order of the two test  
 287 solutes is reversed on the two monolithic columns. On the GMA-co-EDMA monolith, thiourea elutes  
 288 at the hold-up time, while octylbenzene, which is more hydrophobic, elutes with a retention factor of  
 289 approximately 1. This separation takes place according to a reversed-phase mechanism. On the GMA-  
 290 co-MBA monolith and with the same mobile phase, the elution order is reversed, *viz* octylbenzene  
 291 elutes first, indicative of a HILIC separation mechanism. Such a modification of the retention  
 292 mechanism clearly reflects the highly hydrophilic character of this new GMA-co-MBA monolith  
 293 stationary phase.

294 To investigate the benefits of this new monolith on non-specific interactions, the retention factors of  
 295 the 41 fragment-like compounds were measured by nano-FAC on reduced aldehyde GMA-co-MBA  
 296 monolith (GMA-co-MBA\*) and compared with those obtained on reduced aldehyde GMA-co-EDMA  
 297 monolith (GMA-co-EDMA\*) (figure 2, right). As for the first study on GMA-co-EDMA monoliths all this  
 298 set of experiments was carried out in a purely aqueous mobile phase buffered at pH=7.4. For most  
 299 compounds, the non-specific interactions are drastically reduced. The higher the hydrophobic  
 300 character of the solute, the higher the reduction of non-specific interactions. Figure 4 illustrates the  
 301 impact of the reduction of the non-specific interaction for the ligand F366.



302

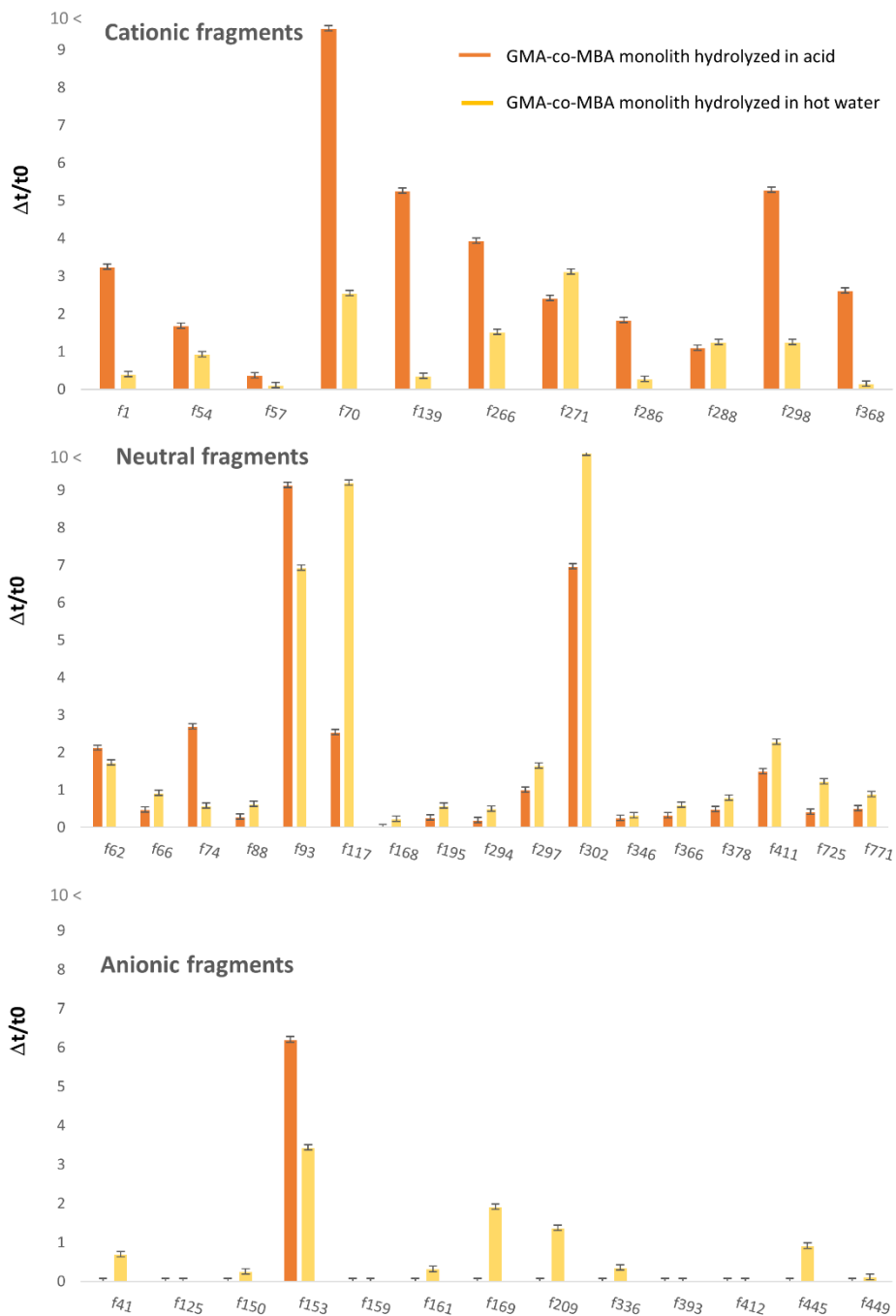
303 Figure 4. Nano-Frontal affinity chromatograms of the molecule F366 on the GMA-co-EDMA\* and GMA-  
 304 co-MBA\* monolith. UV detection at 280 nm, mobile phase sodium acetate 20mM pH 7.4.

305

306 However, this effect observed for hydrophobic neutral compounds must be qualified by the increase  
 307 in retention for some cationic compounds. This unexpected side effect on cationic compounds led us  
 308 to seek its origin. A systematic investigation of the non-specific interactions observed for cationic  
 309 compounds was performed at the different stages of functionalization. This non-specific interactions  
 310 with cationic compounds appear from the first acid hydrolysis step. One hypothesis is the potential  
 311 degradation of the acrylamide functions into carboxylic acids [22]. An alternative hydrolysis route to  
 312 acid hydrolysis has therefore been evaluated to avoid this side-effect. A hot water hydrolysis step was  
 313 therefore studied [23,24].

### 314 3.3 Optimization of the GMA-co-MBA monolith preparation: hot water hydrolysis

315 Following the reported procedures, GMA-co-MBA monolithic capillary columns were subjected to  
 316 thermal treatment in hot water at 80°C for 18 h before undergoing the subsequent streptavidin  
 317 grafting step. The efficiency of this hydrolysis of the epoxide groups method was evaluated through  
 318 the determination of the quantity of grafted protein after the overall process. An amount of  
 319 streptavidin binding sites of  $16 \pm 0.8 \text{ pmol cm}^{-1}$  was obtained. While longer than acidic hydrolysis, this  
 320 milder method using hot water is also effective to prepare affinity columns. To determine the impact  
 321 of such modification on the physico-chemical properties of the resulting monolith, the retention  
 322 behavior of the 41 ligands on reduced aldehyde GMA-co-MBA\* monolith prepared by hot water  
 323 hydrolysis was compared to those obtained by acidic hydrolysis. Figure 5 compares the reduced  
 324 breakthrough times measured on the two GMA-co-MBA\* monoliths. For clarity purpose, the ligands  
 325 were classified by charge state (anionic, neutral and cationic ligands).



326

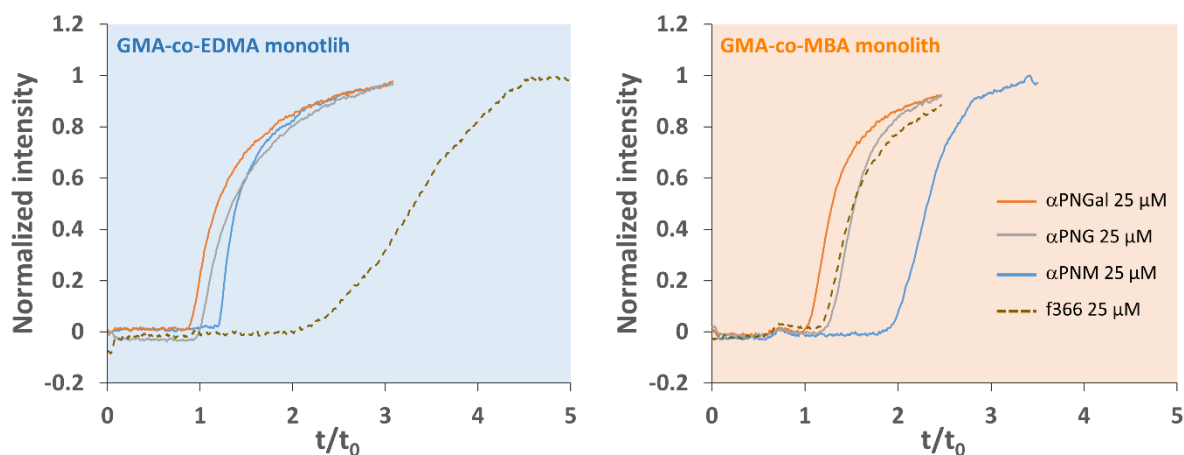
327 Figure 5. Bar graphs of the breakthrough times for the 41 molecules (classified according to their global  
 328 charge: anionic, cationic or neutral fragments) on reduced aldehyde GMA-co-MBA\* monolith  
 329 hydrolyzed in acid (orange) and reduced aldehyde GMA-co-MBA\* monolith hydrolyzed in hot water  
 330 (yellow).

331 Regarding cationic fragments, except for compound f221 that is not affected, the hot water hydrolysis  
332 drastically reduced the level of non-specific interactions observed by nano-FAC experiments.  
333 Meanwhile, this new preparation method has not significantly modified the retention factor for neutral  
334 ligands, except for f117 and f302 for unknown reason. On the contrary, the retention of anionic ligands  
335 slightly increased. The very low level of retention of anionic ligands on the GMA-co-MBA\* monolith  
336 prepared by acid hydrolysis seems to be stressed by repulsive ionic interactions between species of  
337 the same charge. Hydrolysis in hot water is intended to suppress the presence of anionic charge on the  
338 support. In return, the level of retention of anionic ligands slightly increases. The modification of the  
339 physico-chemical properties of the monolith generated by the modification of the mode of hydrolysis  
340 seems to confirm the initial hypothesis according to which the high level of retention for the cationic  
341 ligands came from the presence of negatively charged groups created during the acidic hydrolysis step.  
342 In addition to graft as much as protein than with the previous one, this new hydrolysis method  
343 drastically reduced the level of non-specific interactions for the cationic ligands without affecting the  
344 non-specific interactions for the neutral and anionic ligands. The stability of this GMA-co-MBA  
345 monolith hydrolyzed in hot water was evaluated. The retention factors remained constant for the  
346 duration of use (one week of continuous use) and even after 3 additional months of storage (the  
347 column was store in aqueous solution at room temperature).

#### 348 3.4 Application of the new GMA-co-MBA monolithic affinity columns for the measurement of protein 349 (Con A)-ligand interactions

350 Use of FAC for ligand screening generally relies on the comparison of breakthrough curves of a set of  
351 compounds using a protein immobilized on the stationary phase. Working at a fixed ligand  
352 concentration, the longer the breakthrough time, the higher the affinity. This straightforward  
353 relationship turns out to be more complex when non-specific interactions are not negligible. It is  
354 therefore necessary to find methodological strategies to avoid misinterpretation. For example, it is  
355 possible to use control columns without protein to assess the retention level due to non-specific  
356 interactions on the stationary phase itself. Minimizing the non-specific interactions is necessary both  
357 for reducing the duration of experiments and limiting false positives. To illustrate the impact of non-  
358 specific interactions during screening experiments and show the improvement in the use of a  
359 stationary phase that limits non-specific contributions, nano-FAC experiments were performed on  
360 GMA-co-EDMA and GMA-co-MBA monoliths. Concanavalin A, a lectin that binds mannose-containing  
361 ligands with high affinity, or other carbohydrates with lower affinities [25–27], was used as protein  
362 model. Four ligands were used to illustrate the impact of the non-specific interactions when screening  
363 ligand by nano-FAC. P-nitro- $\alpha$ -D-mannopyranoside ( $\alpha$ PNM) and P-nitro- $\alpha$ -D-glucopyranoside ( $\alpha$ PNG)

364 were used as low affinity ligands (Kd values of 50  $\mu$ M and > 200  $\mu$ M, respectively [27]) and P-nitro- $\alpha$ -  
365 D-galactopyranoside ( $\alpha$ PNGal) and f366 were used as controls (non-ligands).



366

367 Figure 6. Nano-Frontal affinity chromatograms of  $\alpha$ PNM,  $\alpha$ PNG,  $\alpha$ PNGal and the molecule f366 on the  
368 GMA-co-EDMA and GMA-co-MBA monolith. UV detection at 240 nm for the molecule f366 and 300  
369 nm for  $\alpha$ PNM,  $\alpha$ PNG and  $\alpha$ PNGal. Mobile phase sodium acetate 20mM pH 7.4.

370

371 Figure 6 shows the frontal affinity chromatograms obtained for the 4 tested ligands on both stationary  
372 phases. Regarding the glycosides residues, the galactose residue ( $\alpha$ PNGal) as a non-ligand of ConA  
373 elutes early followed by  $\alpha$ PNG and  $\alpha$ PNM) on the two columns. These stereoisomers of monoglycoside  
374 share comparable physico-chemical properties and are highly polar compounds. This supports the  
375 observed behavior of  $\alpha$ PNGal that elutes at the hold-up time of the column ( $t/t_0=1$ ). The order of  
376 elution follows the affinity of the three ligands. The situation is more complex if we look to the more  
377 hydrophobic ligand f366. On the GMA-co-EDMA column, this ligand elutes in last position while it  
378 elutes with  $\alpha$ PNGal on the MBA-co-EDMA column. F366 is a neutral and moderately nonpolar  
379 compound ( $\log D = 0.97$  at pH 7.4). Interpretation of the raw breakthrough curves on the GMA-co-  
380 EDMA monolith would lead to a wrong conclusion about the affinity of the ligands for f366. Conversely,  
381 the use of the highly polar GMA-co-MBA column allows to conserve the order of elution logical with  
382 respect to the ligand affinity. Moreover, the higher amount of active ConA grafted on the monolith  
383 allows a better discrimination between solutes with different Kd values.

384

385 4- Conclusions



386 In affinity chromatography, non-specific interactions between the ligands and the chromatographic  
387 support may affect the results, leading to misinterpretations during the investigation of protein-ligand  
388 interactions (detection of false positives in ligand screening, lack of specificity in purification).  
389 Optimizing the underlying support of the affinity column to reduce nonspecific interactions is an  
390 ongoing goal. A new methodology was first proposed for the characterization of non-specific  
391 interactions. This methodology relies on the determination of the retention behavior of a set of 41  
392 selected small molecules. Such methodology applied to GMA-co-EDMA monolithic capillary columns  
393 has shown that non-specific interactions are mainly due to hydrophobic effects and must be taken into  
394 account. This led us to propose the modification of the monolith synthesis by using MBA crosslinker to  
395 increase the hydrophilicity of the resulting monolith. A large reduction of non-specific interactions was  
396 observed for all the ligands excepted the cationic ones. This behavior of cationic solutes has been  
397 attributed to electrostatic interactions with the monolith after the acidic hydrolysis step (side reaction  
398 onto the MBA crosslinker). Acidic hydrolysis was successfully replaced by a hot water treatment. The  
399 new poly(GMA-co-MBA) monolith not only exhibits improved hydrophilic surface properties, but also  
400 higher protein density ( $16\pm 0.8$  pmol  $\text{cm}^{-1}$  instead of  $8\pm 0.3$  pmol  $\text{cm}^{-1}$  for the GMA-co-EDMA monolith).  
401 The new highly hydrophilic monolith should find applications in various fields of affinity  
402 chromatography (e.g., sample purification, preconcentration, chiral separation, IMERs ...).

403

#### 404 Acknowledgements

405 The author(s) acknowledge(s) the support of the French Agence Nationale de la Recherche (ANR),  
406 under grant ANR-21-CE29-0012 (project NanoWAC).

#### 407 References

- 408 [1] Z. Li, E. Rodriguez, S. Azaria, A. Pekarek, D.S. Hage, Affinity monolith chromatography: A review  
409 of general principles and applications, *ELECTROPHORESIS*. 38 (2017) 2837–2850.  
410 <https://doi.org/10.1002/elps.201700101>.
- 411 [2] E. Calleri, S. Ambrosini, C. Temporini, G. Massolini, New monolithic chromatographic supports  
412 for macromolecules immobilization: Challenges and opportunities, *Rev. Pap. Pharm. Biomed. Anal.*  
413 2012. 69 (2012) 64–76. <https://doi.org/10.1016/j.jpba.2012.01.032>.
- 414 [3] E.L. Pfaunmiller, M.L. Paulemond, C.M. Dupper, D.S. Hage, Affinity monolith chromatography: a  
415 review of principles and recent analytical applications, *Anal. Bioanal. Chem.* 405 (2013) 2133–2145.  
416 <https://doi.org/10.1007/s00216-012-6568-4>.
- 417 [4] H.M. Almughamsi, M.K. Howell, S.R. Parry, J.E. Esene, J.B. Nielsen, G.P. Nordin, A.T. Woolley,  
418 Immunoaffinity monoliths for multiplexed extraction of preterm birth biomarkers from human blood

419 serum in 3D printed microfluidic devices, *Analyst*. 147 (2022) 734–743.  
420 <https://doi.org/10.1039/D1AN01365C>.

421 [5] S. Jiang, Z. Zhang, L. Li, A one-step preparation method of monolithic enzyme reactor for highly  
422 efficient sample preparation coupled to mass spectrometry-based proteomics studies, *J Chromatogr*  
423 *A*. 1412 (2015) 75–81. <https://doi.org/10.1016/j.chroma.2015.07.121>.

424 [6] J. Guo, Q. Wang, D. Xu, J. Crommen, Z. Jiang, Recent advances in preparation and applications of  
425 monolithic chiral stationary phases, *TrAC Trends Anal. Chem.* 123 (2020) 115774.  
426 <https://doi.org/10.1016/j.trac.2019.115774>.

427 [7] L. Lecas, J. Randon, A. Berthod, V. Dugas, C. Demesmay, Monolith weak affinity chromatography  
428 for  $\mu\text{g}$ -protein-ligand interaction study, *J. Pharm. Biomed. Anal.* 166 (2019) 164–173.  
429 <https://doi.org/10.1016/j.jpba.2019.01.012>.

430 [8] L. Lecas, L. Hartmann, L. Caro, S. Mohamed-Bouteben, C. Raingeval, I. Krimm, R. Wagner, V.  
431 Dugas, C. Demesmay, Miniaturized weak affinity chromatography for ligand identification of  
432 nanodiscs-embedded G-protein coupled receptors, *Anal. Chim. Acta.* 1113 (2020) 26–35.  
433 <https://doi.org/10.1016/j.aca.2020.03.062>.

434 [9] D.N. Gunasena, Z. El Rassi, Hydrophilic diol monolith for the preparation of immuno-sorbents at  
435 reduced nonspecific interactions, *J. Sep. Sci.* 34 (2011) 2097–2105.  
436 <https://doi.org/10.1002/jssc.201100353>.

437 [10] S. Khadka, Z. El Rassi, Postpolymerization modification of a hydroxy monolith precursor. Part III.  
438 Activation of poly(hydroxyethyl methacrylate-co-pentaerythritol triacrylate) monolith with epoxy  
439 functionalities followed by bonding of glycerol, polyamines, and hydroxypropyl- $\beta$ -cyclodextrin for  
440 hydrophilic interaction and chiral capillary electrochromatography, *ELECTROPHORESIS*. 37 (2016)  
441 3178–3185. <https://doi.org/10.1002/elps.201600326>.

442 [11] F. Svec, Porous polymer monoliths: Amazingly wide variety of techniques enabling their  
443 preparation, *Ed. Choice IV*. 1217 (2010) 902–924. <https://doi.org/10.1016/j.chroma.2009.09.073>.

444 [12] M. Vergara-Barberán, E.J. Carrasco-Correa, M.J. Lerma-García, E.F. Simó-Alfonso, J.M. Herrero-  
445 Martínez, Current trends in affinity-based monoliths in microextraction approaches: A review, *Anal.*  
446 *Chim. Acta.* 1084 (2019) 1–20. <https://doi.org/10.1016/j.aca.2019.07.020>.

447 [13] M.B. Espina-Benitez, J. Randon, C. Demesmay, V. Dugas, Development and application of a new  
448 in-line coupling of a miniaturized boronate affinity monolithic column with capillary zone  
449 electrophoresis for the selective enrichment and analysis of cis-diol-containing compounds, *J.*  
450 *Chromatogr. A*. 1494 (2017) 65–76. <https://doi.org/10.1016/j.chroma.2017.03.014>.

451 [14] M.B. Espina-Benitez, F. Marconi, J. Randon, C. Demesmay, V. Dugas, Evaluation of boronate  
452 affinity solid-phase extraction coupled in-line to capillary isoelectric focusing for the analysis of

453 catecholamines in urine, *Anal. Chim. Acta.* 1034 (2018) 195–203.  
454 <https://doi.org/10.1016/j.aca.2018.06.017>.

455 [15] J.C. Masini, F. Svec, Porous monoliths for on-line sample preparation: A review, *Anal. Chim. Acta.*  
456 964 (2017) 24–44. <https://doi.org/10.1016/j.aca.2017.02.002>.

457 [16] M. Nechvátalová, J. Urban, Current trends in the development of polymer-based monolithic  
458 stationary phases, *Anal. Sci. Adv.* 3 (2022) 154–164. <https://doi.org/10.1002/ansa.202100065>.

459 [17] S. Poddar, S. Sharmeen, D.S. Hage, Affinity monolith chromatography: A review of general  
460 principles and recent developments, *ELECTROPHORESIS.* 42 (2021) 2577–2598.  
461 <https://doi.org/10.1002/elps.202100163>.

462 [18] A. Gottardini, C. Netter, V. Dugas, C. Demesmay, Two Original Experimental Setups for  
463 Staircase Frontal Affinity Chromatography at the Miniaturized Scale, *Anal. Chem.* 93 (2021) 16981–  
464 16986. <https://doi.org/10.1021/acs.analchem.1c04772>.

465 [19] G. Zhu, H. Yuan, P. Zhao, L. Zhang, Z. Liang, W. Zhang, Y. Zhang, Macroporous polyacrylamide-  
466 based monolithic column with immobilized pH gradient for protein analysis, *ELECTROPHORESIS.* 27  
467 (2006) 3578–3583. <https://doi.org/10.1002/elps.200600189>.

468 [20] R. Mallik, D.S. Hage, Affinity monolith chromatography, *J. Sep. Sci.* 29 (2006) 1686–1704.  
469 <https://doi.org/10.1002/jssc.200600152>.

470 [21] T. Jiang, R. Mallik, D.S. Hage, Affinity Monoliths for Ultrafast Immunoextraction, *Anal. Chem.* 77  
471 (2005) 2362–2372. <https://doi.org/10.1021/ac0483668>.

472 [22] Y. Pei, L. Zhao, G. Du, N. Li, K. Xu, H. Yang, Investigation of the degradation and stability of  
473 acrylamide-based polymers in acid solution: Functional monomer modified polyacrylamide,  
474 *Petroleum.* 2 (2016) 399–407. <https://doi.org/10.1016/j.petlm.2016.08.006>.

475 [23] Z. Wang, Y.-T. Cui, Z.-B. Xu, J. Qu, Hot Water-Promoted Ring-Opening of Epoxides and Aziridines  
476 by Water and Other Nucleophiles, *J. Org. Chem.* 73 (2008) 2270–2274.  
477 <https://doi.org/10.1021/jo702401t>.

478 [24] L.P.D. Ratcliffe, A.J. Ryan, S.P. Armes, From a Water-Immiscible Monomer to Block Copolymer  
479 Nano-Objects via a One-Pot RAFT Aqueous Dispersion Polymerization Formulation, *Macromolecules.*  
480 46 (2013) 769–777. <https://doi.org/10.1021/ma301909w>.

481 [25] K. KASAI, Frontal affinity chromatography: A unique research tool for biospecific interaction that  
482 promotes glycobiology, *Proc. Jpn. Acad. Ser. B Phys. Biol. Sci.* 90 (2014) 215–234.  
483 <https://doi.org/10.2183/pjab.90.215>.

484 [26] K. Kasai, Frontal affinity chromatography: An excellent method of analyzing weak biomolecular  
485 interactions based on a unique principle, *Biochim. Biophys. Acta BBA - Gen. Subj.* 1865 (2021) 129761.  
486 <https://doi.org/10.1016/j.bbagen.2020.129761>.

487 [27] Y. Oda, K. Kasai, S. Ishii, Studies on the Specific Interaction of Concanavalin A and Saccharides by  
488 Affinity Chromatography. Application of Quantitative Affinity Chromatography to a Multivalent  
489 System, J. Biochem. (Tokyo). 89 (1981) 285–296.  
490 <https://doi.org/10.1093/oxfordjournals.jbchem.a133192>.  
491